Brønsted and Lewis Acid Sites in Dealuminated ZSM-12 and β Zeolites Characterized by NH_3-STPD, FT-IR, and MAS NMR Spectroscopy

Wenmin Zhang,[†] Panagiotis G. Smirniotis,*[,†] M. Gangoda,[‡] and Rathindra N. Bose*[,‡]

Department of Chemical Engineering, University of Cincinnati, Cincinnati, Ohio, 45221-0171, and Department of Chemistry, Kent State University, Kent, Ohio 44240

Received: August 31, 1999; In Final Form: February 1, 2000

Infrared spectroscopy, nuclear magnetic resonance, and NH_3-stepwise temperature-programmed desorption (STPD) were used to study the acidity characteristics of dealuminated ZSM-12 and β zeolites in a wide range of Si/Al ratios. For all samples, the STPD experiments revealed the presence of five distinct peaks. A 1:1 relation between the Al atoms of each sample and ammonia determined from the STPD experiments was derived, thus indicating that this technique can probe accurately all acid sites for zeolites with Si/Al $\geq$ about 20. A careful deconvolution of the FT-IR peaks indicated that only the as-synthesized ZSM-12 sample possessed a small number of Lewis acid sites. We found that ammonia desorbs completely from those Lewis sites upon an increase of temperature above 150 °C. It is remarkable to note that all the dealuminated ZSM-12 samples do not possess any Lewis acid sites. This is in contrast to what is commonly known since during dealumination framework aluminun atoms move to extraframework locations. It seems that during the dealumination of ZSM-12 the acid "washes" all the extraframework Al atoms. This was not the case for β zeolite since the as-synthesized and dealuminated β zeolites with Si/Al $\leq$ 80 possess Lewis sites. By coupling results from the NH_3-STPD and FT-IR studies, we found that the Lewis sites of β zeolites are of weak strength since chemisorbed ammonia does not remain on those sites at temperatures higher than about 300 °C. These results are in very good agreement with the Al-27 NMR data which indicate mostly the presence of tetrahedral sites for ZSM-12; an extremely small abundance of octahedral sites were detected only with Si/Al ratios < 40. Si-29 NMR data can be described by at least three distinctly different Si sites. On the basis of the chemical shift and intensity distribution data, two of these sites can be assigned to Q^4 and the remaining Si site is consistent with being a Q^3 site. For β zeolite Al-27 NMR spectra show a relatively high concentration of octahedral sites, thus supporting the presence of Lewis sites. Furthermore, the NMR peaks for the tetrahedral sites in β zeolite are asymmetric and broad compared to ZSM-12 samples, indicating the presence of two or more different tetrahedral or distorted tetrahedral sites. The Si-29 NMR spectra of β zeolite are qualitatively similar to those observed for the ZSM-12 samples.

Introduction

The acidity characteristics of zeolites play an important role in their performance both as catalytic materials and as sorbents. In addition to the Si/Al ratio, which describes the acid sites density, information on the nature of Al sites, i.e., framework and nonframework species, and the strength distribution is needed. The nature and strength distribution can significantly vary with the aluminum content and the method of dealumination. Spectroscopic techniques such as FT-IR and MAS NMR have been used for qualitative and quantitative characterization of acid sites in zeolites. The former method relies on infrared bands associated with the interaction of a probe base with Brønsted and Lewis acid sites, while the latter deals with the nature of the coordination sphere of Al and Si in zeolites. More specifically, tetrahedrally coordinated Al species are Brønsted sites, while those in octahedral environments are known as Lewis sites. Both tetrahedral and octahedral sites are readily resolved by Al-27 NMR due to their distinctly different chemical shifts. In addition to these tetrahedral and octahedral sites, others[1] reported that, in β zeolite, NMR-invisible aluminum may exist under specific treatment conditions. These NMR-invisible Al sites were thought to have significantly distorted tetrahedral geometry and are associated with a strongly acidic hydroxyl group with IR vibrations at about 3780 cm^{-1}. Furthermore, those researchers concluded that NMR-invisible Al sites constitute the framework species. A third type of Al site was referred by others[2] in dealuminated USYs which are associated with the steam dealumination of the samples. In a recent work dealing with ZSM-5, others[3] observed no octahedral aluminum by NMR, while TPD and FT-IR experiments indicated the existence of Lewis acidity. Other researchers[4] found that the increase of the dealumination results in the migration of tetrahedrally coordinated lattice Al(IV) atoms (Brønsted sites) to octahedrally coordinated positions, Al(VI). Evidently, the dealumination method (chemical agent, severity, specific conditions) results in unexpected trends for the acidic properties of zeolites.

In this paper we investigate the acidity characteristics of dealuminated ZSM-12 and β zeolite in an attempt to address the nature, type, and strength of acid sites as a function of dealumination. Both zeolites are 12-membered ring pore, high-silica zeolites that are very important for several industrial applications. FT-IR and MAS NMR spectroscopic techniques were used to address the coordination environments of Al and

* To whom correspondence should be addressed.
[†] University of Cincinnati.
[‡] Kent State University.

10.1021/jp993072p CCC: $19.00
Published on Web 04/01/2000

TABLE 1: Properties of the Zeolite Samples Studied

sample	HCl concn (N)	Si/Al (bulk)	crystallinity (%)
ZSM-12	as-synthesized	34.5	100
ZSM-12/1	1.0	40	~100
ZSM-12/2	2.0	47	~100
ZSM-12/3	3.0	54	~100
ZSM-12/4	4.0	58	~100
ZSM-12/5	5.0	69	~100
β	as-synthesized	14.5	100
β1	0.2	58	89
β2	2.5	70	77
β3	5.0	85	79
β4	7.0	132	90

Si sites, while stepwise temperature-programmed desorption (STPD) of NH_3 was used to quantify the amount of the base desorbing from Brønsted and Lewis acidic sites of different strengths.

Experimental Section

Zeolite synthesis. The parent ZSM-12 and β zeolites were hydrothermally synthesized from the corresponding aluminosilicate gels with nominal compositions $88SiO_2$:Al_2O_3:$6.6Na_2O$:$13TEABr$:$900H_2O$ (where TEABr stands for tetraethylammonium bromide) and $30SiO_2$:Al_2O_3:$0.9Na_2O$:$3TEAOH$:$250H_2O$ (where TEAOH stands for tetraethylammonium hydroxide), respectively. The gels were prepared from the individual solutions in the appropriate proportions and then were loaded into a Teflon-lined autoclave. The synthesis took place at 150 °C and autogenous pressure, and the crystallization period was 40 and 10 days, respectively. The as-synthesized zeolites were calcined in air at 530 °C for 4 h to burn the occluded template. X-ray experiments showed that the zeolites were highly crystalline. Different concentrations of HCl were used for the preparation of dealuminated samples, which was carried out in a 1 L three-neck flask under reflux at 90 ± 1 °C for 4 h. For each batch 2 g of template-free zeolite was used. After the end of the dealumination step the contents of the flask were filtered, washed thoroughly with distilled water, and dried overnight. The bulk Si/Al ratio of the dealuminated zeolites was determined with ICP spectroscopy (LEEMAN LAB ICP2.5) after each sample was fused at 900 °C in the presence of lithium metaborate. The relative decrease of crystallinity was determined with XRD analysis utilizing a Siemens D500 diffractometer with a Cu K_α source. The properties of the samples studied in the present paper are presented in Table 1. The protonated form of the samples was obtained by cation exchanging the samples of various Si/Al ratios with a 2.0 M NH_4Cl solution under reflux. Finally, the samples were calcined in air at 450 °C for 1 h.

NH_3-STPD and FT-IR Studies. The NH_3-STPD experiments were successfully performed in our earlier work[5] for the quantitative determination of the ammonia desorbing from acid sites of different types and strengths. In contrast to the traditional temperature-programmed desorption experiments, which are carried out with a constant heating rate, we utilize an optimized temperature heating profile which consists of combinations of isothermal steps followed by steps of constant heating rate. In this manner, we are able to generate very reproducibly individual desorption peaks which result from Lewis or Brønsted or from both Lewis and Brønsted acid sites of different strengths. The desorption profile was generated by a thermal conductivity detector. A 50 mg portion of each sample was loaded into the reactor and "cleaned" by purging with helium at 550 °C. The adsorption of anhydrous ammonia (3.89% in helium) was carried out at 150 °C for several hours. The latter step ensured that there is no contribution to the desorption from physisorbed ammonia.[6] The STPD experiments were performed in the range of 150−550 °C and gave five distinct peaks. The experiments were repeated several times, and high reproducibility was achieved.

For the FT-IR experiments self-supported wafers were made by pressing (5000 lb) about 9 mg of the protonated form of the zeolite. The synthesized wafer was 9 mm wide and about 40 μm thick, something that ensured minimum reduction of the IR beam intensity. The wafer was placed in a handmade bakeable IR cell with CaF_2 windows. Prior to the runs, each sample was purged in helium and kept at 550 °C for 1 h. Higher temperatures were not used in order to avoid the crystallographic degradation of the zeolite structure as well as the dehydration of the zeolite associated with the transformation of Brønsted to Lewis sites. During the cooling cycle to 150 °C, anhydrous ammonia was admitted to the sample for sufficient time to allow complete saturation of all the sites. Prior to the collection of the data the purging of the sample with helium at 150 °C was applied to remove physisorbed ammonia. The samples were heated to the appropriate temperature ranging from 150 to 550 °C to simulate the exact desorption conditions applied during the STPD experiments. The IR transmission spectra were collected on a Bio-Rad FTS-40 spectrometer always at 150 °C after the wafer was cooled from the desired desorption temperature. The collection of the IR spectra was performed at the same temperature to determine accurately the extinction coefficients for Brønsted and Lewis sites which are sensitive to the temperature of the wafer. Scans were taken by using open aperture with a sensitivity of 8. Sixteen scans with a resolution of 2 cm^{-1} were used. The qualitative description of the Lewis and Brønsted acid sites was based on the IR bands in the range of 1700−1400 cm^{-1}. The peaks at 1625 and 1454 cm^{-1} were used for the Lewis and Brønsted sites, respectively. For this reason, deconvolution of the broad peak occurring at about 1640 cm^{-1} was performed to separate the Lewis band from the peak which corresponds to the structural vibrations of the zeolites in this region. The deconvolution procedure was applied for other regions of the FT-IR experiments to decouple multiple peaks. For the deconvolution the curvefit subroutine of the Win-IR software package was used to assign individual peaks of Gaussian shape in each range of interest. The R^2 correlation coefficient for each deconvolution was always larger than 99%.

Al-27 and Si-29 NMR Studies. Aluminum-27 and silicon-29 NMR spectra were recorded on a wide-bore NMR instrument (Bruker 400 DMX) operating at 9.4 T. XWINNMR software operating in a Unix environment on a Silicon Graphics computer (Indy) was employed to acquire and retrieve data. Aluminum-27 spectra were acquired at 104.3 MHz with a sweep width of 31.5 kHz by using 1K data points. For the high-power one-pulse experiments, typically, a 1 μs pulse (flip angle 18°) with a pulse repetition time of 1 s was used. Samples were loaded onto 7 mm zirconia rotors which were spun at a speed of 2−3 kHz. The spectra were externally referenced with respect to a dilute solution of $AlCl_3$ at 0.0 ppm.

Silicon-29 spectra were recorded at 79.5 MHz. Typical data acquisition parameters were 90° pulse of 2−4 μs duration, 3 μs pulse repetition time, 1K data points, and 0.21 s data acquisition time. For the CP-MAS experiments, the typical data acquisition parameters were 90° proton pulse of 4 μs duration, 250 kHz decoupling frequency, 6.5 ms contact time, and a pulse repetition delay of 2 s. This contact time fulfills the requirement of Hartmann−Hahn polarization transfer of SiOH groups which was determined experimentally by a series of experiments. In

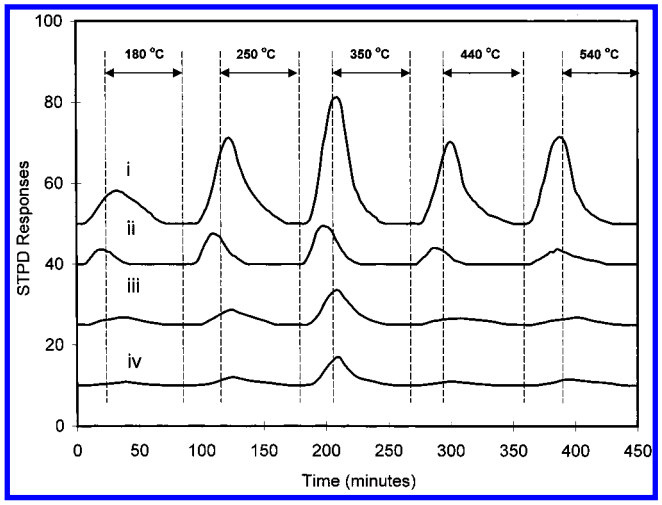

Figure 1. NH_3-stepwise temperature-programmed desorption profiles of β zeolite samples with (i) Si/Al = 14.5 and (ii) Si/Al = 70 and ZSM-12 samples with (iii) Si/Al = 34.5 and (iv) Si/Al = 54.

these experiments, spectra with variable mixing times were recorded and optimum contact time was determined from the intensity vs contact time plot. The chemical shifts are with respect to TMS externally referenced at 0.0 ppm.

The spectra with overlapping peaks were analyzed by the Bruker software. In this deconvolution procedure, the peaks were fitted freely to a number of contributing resonances of Lorenztian distribution. In this computation, line widths, chemical shifts, and percent contributions are varied in an iterative manner, until the convergence criteria are fulfilled, i.e., an excellent agreement between the simulated and calculated peaks is observed.

Results and Discussion

The coupling of NH_3-STPD with FT-IR has been used in our earlier work[5] to provide a qualitative and quantitative measure of the type and strength of acid sites of dealuminated β zeolites. The uniqueness of the STPD in comparison with the conventional TPD experiments is that the former technique allows for the direct separation of ammonia desorption peaks which correspond to different types of acid sites of variable strength. Hence, one can avoid the use of deconvolution techniques which rely on an a priori knowledge of the number of peaks. Others[7] have shown that previous theoretical models[8,9] cannot decouple successfully the typical TPD profiles of acidic catalysts to individual peaks. We found that the desorption profiles obtained with the STPD technique are insensitive to variations in the temperature profile, indicating that the acid sites of ZSM-12 possess distinct limits of strength. The NH_3-STPD experiments with protonated ZSM-12 are presented in Figure 1 for selected Si/Al ratios (curves iii and iv). One can observe that there is a monotonic decrease of the area of all peaks with the increase of the extent of dealumination. The largest peak appears in the medium desorption temperature, and as will be shown below from the FT-IR characterization all the ammonia peaks correspond practically to desorption from Brønsted sites of variable strength. By comparing the NH_3-STPD profiles of all six samples of HZSM-12 involved in the study, we concluded that the peaks shift toward lower temperatures with the increase of the Si/Al ratio. This indicates that the dealumination decreases monotonically the strength of Brønsted sites.

The assignment of the peaks determined from the NH_3-STPD experiments was achieved by performing FT-IR studies at the same temperatures where the ammonia peaks occurred. The IR bands at 1454 and 1625 cm^{-1} correspond to Brønsted (NH_4^+ deformation vibrations) and Lewis acid sites, respectively. One should note (Figure 2a, case i for data recorded at 150 °C) that the latter peak has its maximum at 1640 cm^{-1}. The IR

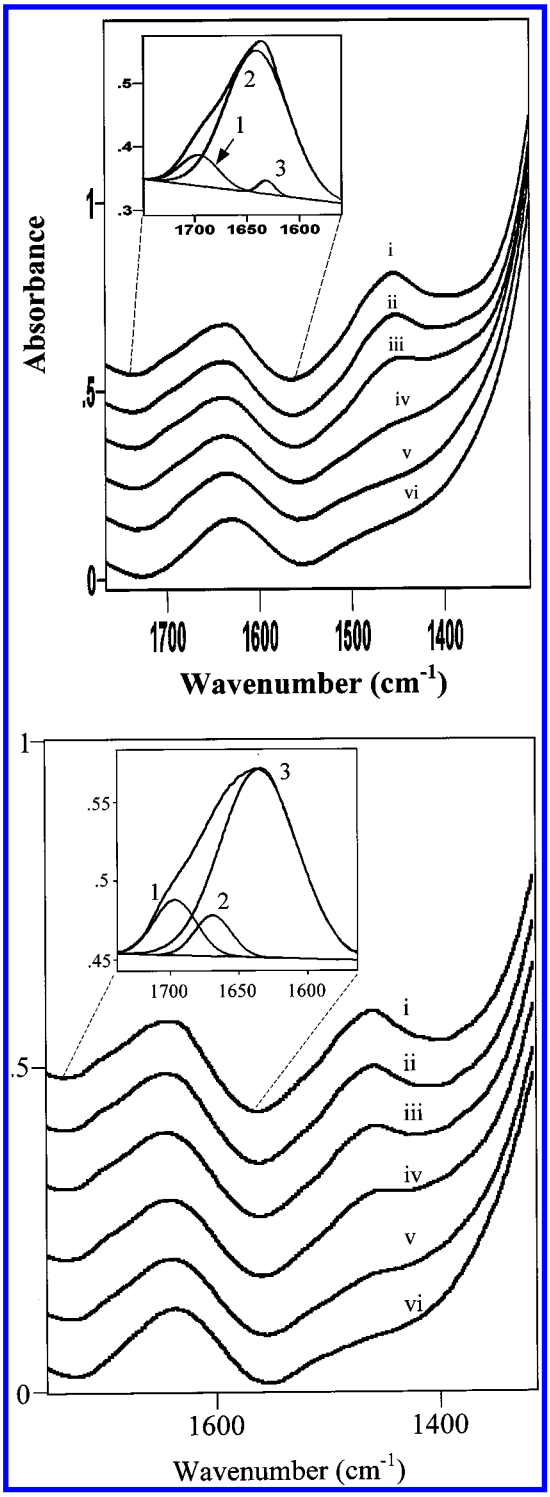

Figure 2. (a, top) FT-IR spectra of nondealuminated HZSM-12 (Si/Al = 34.5) at different desorption temperatures [(i) 150 °C, (ii) 180 °C, (iii) 250 °C, (iv) 350 °C, (v) 440 °C, (vi) 540 °C]. The peaks resulting from the deconvolution are at (1) 1698 cm^{-1}, (2) 1642 cm^{-1}, and (3) 1631 cm^{-1}. (b, bottom) FT-IR spectra of dealuminated HZSM-12 (Si/Al = 54) at different desorption temperatures [(i) 150 °C, (ii) 180 °C, (iii) 250 °C, (iv) 350 °C, (v) 440 °C, (vi) 540 °C]. The peaks resulting from the deconvolution are at (1) 1696 cm^{-1}, (2) 1669 cm^{-1}, and (3) 1635 cm^{-1}.

experiments with NaZSM-12 showed that there is a strong peak at about 1640 cm^{-1} and a smaller one at 1680 cm^{-1} which correspond to vibrations due to the structure of the zeolite. Other zeolites such as Na-mordenite possess an IR band at the same wavenumber.[10] Peak deconvolution allowed us to quantify the real area which corresponds to the ammonia bond on Lewis sites (1625 cm^{-1}). The latter peak disappears with a further increase of temperature. Numerical integration of the band at about 1640 cm^{-1} which corresponds to zeolite vibrations shows that the area does not change (within the experimental error) with the increase of temperature. The magnitude of the latter peaks is large in comparison with that corresponding to the Lewis sites. The increase of temperature (Figure 2a) shows a monotonic decrease of the area of the Brønsted peak (1454 cm^{-1}). The desorption at 540 °C results in complete disappearance of the Brønsted band. The above observations indicate that the desorption peaks of the NH_3-STPD experiments result from ammonia desorbing entirely from Brønsted sites. For ZSM-12 samples of higher Si/Al ratios than the as-synthesized sample (Si/Al = 34.5), no Lewis sites were detected at any desorption temperature (Figure 2b), which is in excellent agreement with the Al-27 investigation presented below. This observation shows that the dealumination of ZSM-12 does not result in an increase of the relative concentration of Lewis sites at the expense of Brønsted ones (a very common observation occurring during dealumination), but in contrast the Lewis sites disappear completely. Others[4] reported that, during the dealumination of zeolites, tetrahedrally coordinated lattice Al(IV) species (Brønsted sites) are removed from the zeolite lattice and migrate to octahedrally coordinated positions (Al(VI)). Dumesic and coworkers[11] observed an increase of the number and strength of Lewis sites by increasing the severity of steam dealumination for USY samples. From the present studies it seems that the acid leaching of the as-synthesized ZSM-12 sample (Si/Al = 34.5) during dealumination causes the "washing" of extraframework aluminum species (Lewis sites). This remarkable observation indicates that the aluminum of ZSM-12 remains as the framework species regardless of the level of dealumination. This is in very good agreement with the preservation of high levels of crystallinity of ZSM-12 after acid leaching (Table 1) even under severe dealumination conditions (5 N HCl).

It should also be noted that the individual peaks determined from the STPD experiments remain unchanged with variations of the temperature profile, thus indicating that zeolites possess distinct limits of strength. This was not the case in our recent work[12] where we studied the acidity of V_2O_5/TiO_2-based catalysts since ammonia was desorbing from both Lewis and Brønsted sites at any temperature regardless of the temperature profile. Quantitative calibration of the NH_3-STPD experiments has shown that for any Si/Al ratio there is a 1:1 relation between the number of Al sites and the total number of ammonia molecules desorbing during each STPD experiment (including five peaks). A similar correlation was observed by others[13] for HZSM-12 utilizing other basic probe molecules (2-propanol, 2-propanamine) where 1:1 adsorption complexes with the acid sites were formed. It is worth noting that the 1:1 relation of NH_3 with the acid sites that we observed from our STPD experiments was true only for zeolites with Si/Al above a certain value. Our recent work[14] shows that, for high-Al-content zeolites such as USY, mordenite, and L, the number of ammonia molecules chemisorbed per acid site is significantly smaller than that for zeolites with high Al density, which does not allow the stoichiometric chemisorption of ammonia.

TABLE 2: Acidic Properties of the ZSM-12 and β Zeolite Samples Studied

Si/Al (bulk)	NH_3 chemisorbed[a]	NH_3/Al	Brønsted sites (mmol/g of catalyst)	Lewis sites (mmol/g of catalyst)
		ZSM-12		
34.5	10.4	0.98	0.39	0.071
40	8.8	0.96	0.39	0.0
47	7.7	0.98	0.34	0.0
54	6.8	0.99	0.30	0.0
58	6.9	1.09	0.31	0.0
69	5.7	1.06	0.25	0.0
		β Zeolite		
14.5	26.4	1.01	0.54	0.56
75.9	5.5	1.06	0.22	0.01
85	4.2	0.91	0.18	0.0
132	2.7	0.94	0.12	0.0

[a] Millimoles of ammonia per gram of zeolite sample under STP conditions.

Additional evidence for the lack of Lewis sites comes from the FT-IR spectra at the hydroxyl stretching vibrations region (3800−3300 cm^{-1}). Chiche et al.[15] found a band at 3780 cm^{-1} which corresponds to hydroxyl groups bound to extraframework aluminum species (Lewis sites). From our experiments (not shown) we did not observe any IR band at this wavenumber, thus indicating the lack of Lewis sites. Hence, the five ammonia desorption peaks of the STPD experiments (Figure 1) are associated primarily with Brønsted sites of variable strength; the higher desorption temperature corresponds to higher acid strength. One can observe that for all the samples the third peak which corresponds to desorption temperatures of about 250 °C is the largest one and represents about 50% of the total area. The concentration of low-temperature peaks (first and second) which correspond to low strength are comparable with that of the peaks which correspond to high strength (high desorption temperature; fourth and fifth peaks).

The numbers of Lewis and Brønsted acid sites for the ZSM-12 samples studied in this work are presented in Table 2. For the determination of these numbers extinction coefficients were estimated by combining results from the STPD and FT-IR experiments. From the desorption experiments above 350 °C we observed repeatedly that ammonia desorbs only from Brønsted sites. Therefore, by combining information from the areas of the STPD and the FT-IR runs, one can determine the extinction coefficient for the Brønsted acid sites. Once this task is completed, one can refer to the low-temperature STPD peaks which contain ammonia desorbing from Lewis sites as well (for ZSM-12 only the as-synthesized sample had a relatively low number of Lewis sites) and therefore record all acid sites.

The STPD profiles for selected samples of β zeolite are presented in Figure 1. The profiles look similar to those of ZSM-12, and the heights of the peaks decrease with the increase of the dealumination severity. At this point we should mention that, as for the case of ZSM-12, the desorption profiles were highly reproducible and are not sensitive to moderate variations of the temperature profile. In contrast to the case of ZSM-12 samples, we observed that the increase of the dealumination increases monotonically the strength of acid sites of β zeolites. We concluded that there is 1:1 relation between Al sites of each β zeolite sample and the total number of ammonia molecules estimated from the STPD experiment. The FT-IR experiments assisted us in identifying the Lewis and Brønsted sites of β zeolites. One can observe (Figure 3a) that the peak at about 1454 cm^{-1} which belongs exclusively to Brønsted sites decreases with the increase of temperature, indicating the gradual

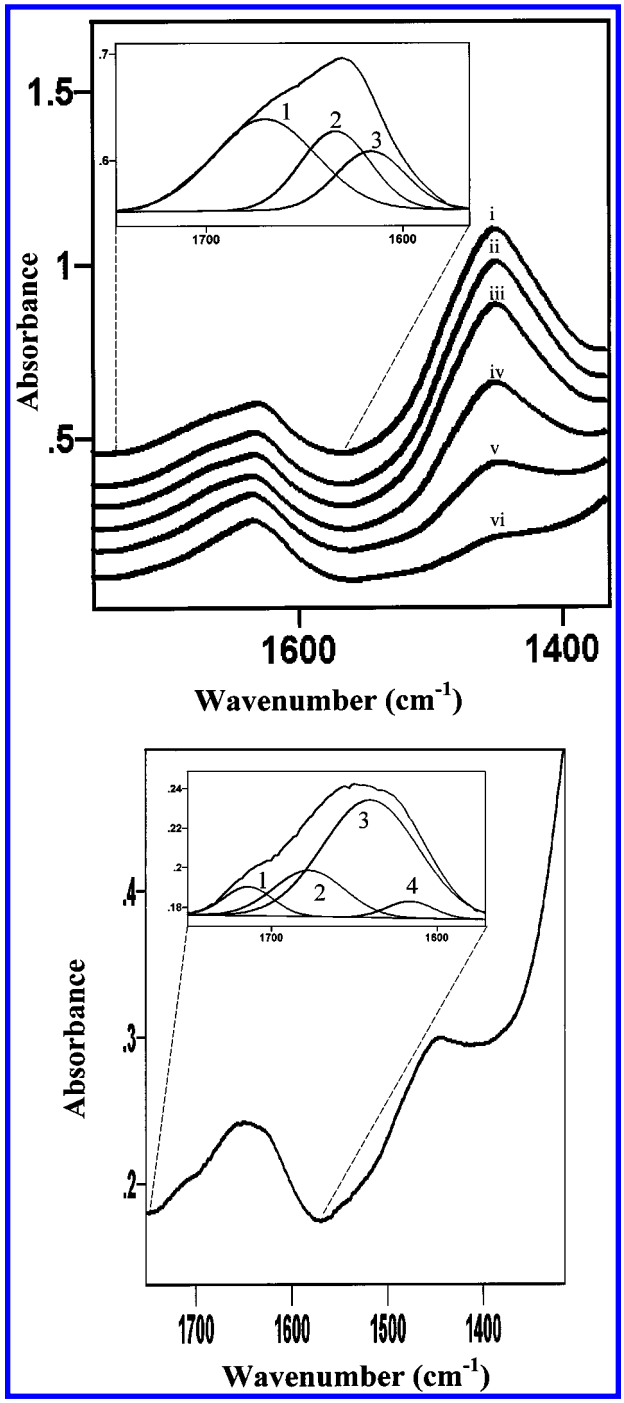

Figure 3. (a, top) FT-IR spectra of nondealuminated β zeolite (Si/Al = 14.5) at different desorption temperatures [(i) 150 °C, (ii) 180 °C, (iii) 250 °C, (iv) 350 °C, (v) 440 °C, (vi) 540 °C]. The peaks resulting from the deconvolution are at (1) 1670 cm^{-1}, (2) 1634 cm^{-1}, and (3) 1616 cm^{-1}. (b, bottom) FT-IR spectra of dealuminated β zeolite (Si/Al = 70) at 150 °C. The peaks resulting from the deconvolution are at (1) 1714 cm^{-1}, (2) 1677 cm^{-1}, (3) 1640 cm^{-1}, and (4) 1616 cm^{-1}.

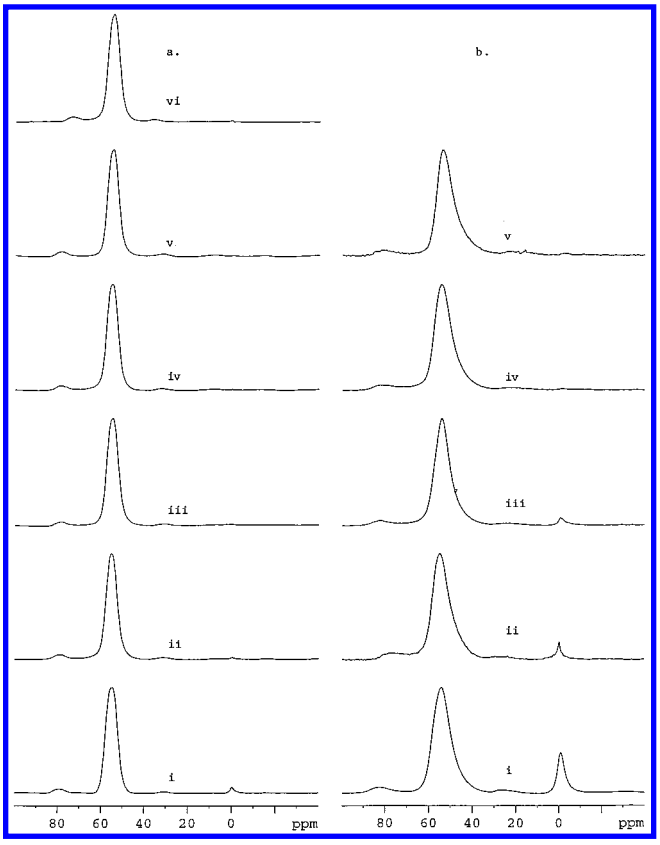

Figure 4. High-resolution MAS Al-27 NMR (104.3 MHz) spectra of ZSM-12 (a) and β zeolites (b) with various Si/Al ratios. These ratios are from bottom to top (a) 34.5 (i), 40 (ii), 47 (iii), 54 (iv), 58 (v), and 69 (vi) and (b) 14.5 (i), 58 (ii), 70 (iii), 85 (iv), and 132 (v).

desorption of ammonia. This peak vanishes completely at elevated temperatures. All β zeolite samples behave in a similar manner in this respect. The deconvolution of the broad peak at about 1640 cm^{-1} reveals the existence of the Lewis peak at 1616 cm^{-1} (peak 3, Figure 3a) and two other peaks at 1670 and 1634 cm^{-1} which correspond to structural vibrations. A careful examination of the deconvoluted peaks showed that the Lewis peak decreases rapidly during heating at the lower temperatures and thus acquires significantly low values at the highest desorption temperatures. This indicates that the low-temperature peaks of the STPD experiment with β zeolites are associated strongly with ammonia desorbing from Lewis sites. The increase of the Si/Al ratio of β zeolites results in a relative decrease of the Lewis peak. A typical example of this trend is presented in Figure 3b for Si/Al = 70 where the height of the Lewis band (peak 4) has been decreased significantly. A new peak at 1714 cm^{-1} (peak 1) has emerged as a result of the acid leaching. This peak is present only in the dealuminated β zeolite samples, including the most highly dealuminated sample with Si/Al of 132. For samples with high Si/Al, namely, 132, no Lewis sites are detected, which agrees very well with the Al-27 NMR results presented below. By using the methodology described above for ZSM-12, we estimated the number of Lewis and Brønsted acid sites for β zeolites as well (Table 2). As expected, a monotonic decrease of the number of Brønsted and Lewis sites is observed with the increase of the Si/Al ratio.

Figure 4a shows Al-27 MAS spectra of protonated ZSM-12 samples with different Si/Al ratios. As can be seen from the figure the samples exhibit a broad peak centered at 55 ppm. In addition, an extremely small peak at 0.0 ppm was observed only for the as-synthesized sample (Si/Al = 34.5). These peaks at 55 and 0.0 ppm are invariably assigned to aluminum centers with tetrahedral and octahedral geometry coordinated through oxygen donor atoms, respectively. Figure 5 shows the molar ratio of octahedral to tetrahedral Al sites as determined from the peak area as a function of Si/Al ratio. Results of similar experiments for β zeolite are exhibited in Figures 4b and 5. Although the results are qualitatively similar, there are some subtle differences between the two zeolites. First, the intensity of aluminum centers in octahedral sites of β zeolite is significantly higher than that for the ZSM-12 samples. In contrast to the β zeolite samples where the dealumination results

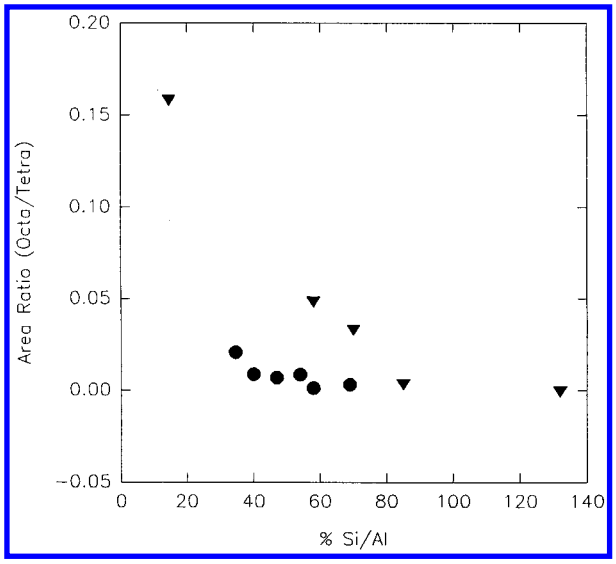

Figure 5. Calculated molar ratios of octahedral/tetrahedral Al vs Si/Al ratio for ZSM-12 (●) and β zeolite (▼) samples indicated in Figure 4.

in formation of octahedral aluminum sites for Si/Al ≤ 70 (compare cases i, ii, and iii with iv or v of Figure 4b), the dealumination of the mother ZSM-12 zeolite results in practically no octahedral sites (compare case i with case ii of Figure 4a). This behavior is in excellent agreement with the FT-IR results for Lewis sites presented in Figures 2 and 3. Second, the line width of the tetrahedral aluminum atoms is substantially larger in the β samples. Furthermore, the line shapes for β samples for the same aluminum centers appear to be skewed and asymmetrical. In fact, these asymmetrical peaks can be deconvoluted into two components (Figure 6) with a $\Delta\nu_{1/2}$ value of 1 (700 ± 50 Hz) comparable to that observed for the ZSM-12 samples (650 ± 25 Hz). The second component has a much larger half-width, 1550 ± 150 Hz. The computer-simulated peaks appear at 54.5 ± 0.5 and 51 ± 1 ppm, the latter being the broader peak. Furthermore, peak areas of the components indicate that they are of equal abundance. The significance of the likelihood of the existence of a broad second peak in the zeolite framework is discussed below. Two additional symmetrical peaks at about 30 and 80 ppm around the central peak were also observed. These two peaks were identified as the spinning sidebands, although these signals match with the reported chemical shifts[4,16,17] of pentacoordinated aluminum species and $Al(OH)_4^-$.

Figure 7a exhibits Si-29 MAS NMR spectra of ZSM-12 zeolite samples. These spectra clearly show evidence for at least three magnetically nonequivalent Si centers by exhibiting well-defined shoulders and peaks. Three component peaks from the overlapping spectra were resolved by computer simulations. Both the simulated and observed spectra for one of the samples are displayed in Figure 8a. As can be seen from Figure 8a, excellent agreement between the observed and simulated spectra was observed. These three components must represent three Si sites in the zeolites. Conventionally, Si sites are labeled as Q^0 through Q^4 corresponding to 4 through 0 Al atoms in the second coordination sphere of Si atoms. Since our Si/Al ratios lie in the range 34.5−132, it is statistically improbable that significant Si atoms are surrounded by more than one Al atom. Assuming that no signals originated from Si sites more than one Al atom in the second coordination sphere, there must be at least one Q^4 site and one Q^3 site in our samples. In principle the third site may be either a second Q^4 or a second Q^3 site due to the defect in the framework or different Al sites as described below.

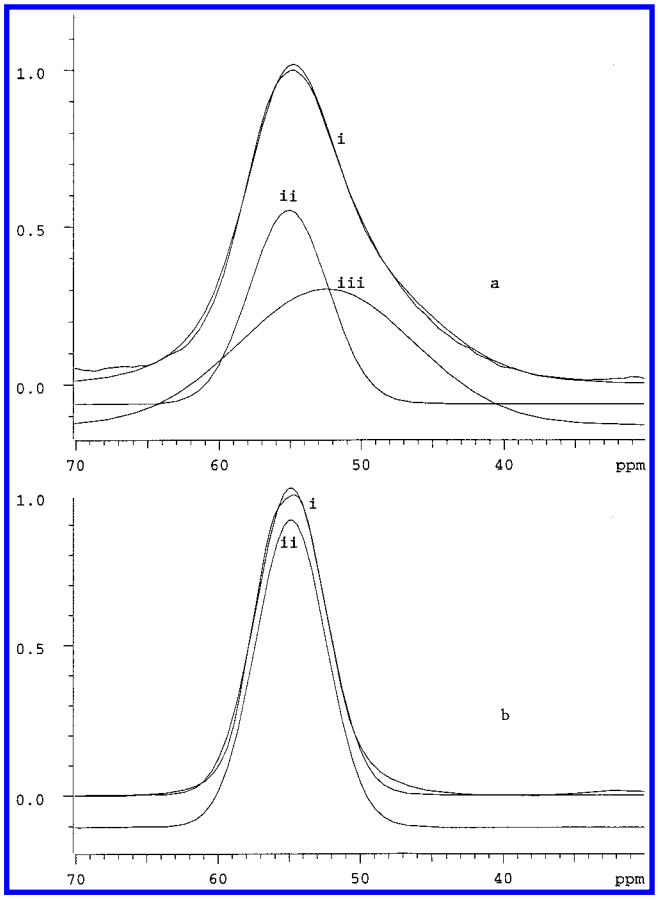

Figure 6. Experimental and simulated MAS Al-27 spectra of β zeolite (a) and ZSM-12 (b) both with Si/Al = 58. Note that at least two components with chemical shifts of 54.5 and 51.0 ppm are required for the simulation of the β zeolite spectrum while the ZSM-12 spectrum can be fitted with one component at 55 ppm only. The simulated and experimental spectra are the two closely matched overlapped peaks abbreviated as i, with the smooth curve being the simulated one, and the calculated component peaks are labeled as ii and iii for β zeolite and ii for the ZSM-12 sample.

Figure 7b shows Si-29 MAS NMR spectra of the β zeolite samples with various Si/Al ratios. The spectra are qualitatively similar to those observed for the ZSM-12 samples in that there are three overlapping peaks in each spectrum. Here again, these signals were resolved into three by the deconvolution procedure stated earlier. Both simulated and observed spectra are displayed in Figure 8a. The chemical shifts of two are close to each other; the difference in chemical shift of these two sites are within 2−3 ppm, while the third one differs from the other two by a minimum of 6 ppm. For example, three deconvoluted peaks for a sample with a Si/Al ratio of 14.5 appear at −111, −109, and −103 ppm. These chemical shift data along with the calculated Si/Al ratio (discussed below) support the presence of two Q^4 sites as opposed to two Q^3 sites.

In principle, taking the areas under the peaks, Si/Al ratios can be calculated. In fact we have used a USY zeolite sample with a Si/Al ratio of 2.6 to calculate the Si/Al ratio from the NMR data. Si-29 NMR data indicate the presence of four peaks at −105, −99, −94, and −89 ppm which can be assigned to Q^4 through Q^1 sites, respectively. On the basis of the peak areas of these four signals, we calculate a Si/Al ratio of 2.5, which is in good agreement with the analytical data of 2.6. We calculated a Si/Al ratio of 16 for the highest Al content (Si/Al = 14.5) by assuming two Q^4 sites and one Q^3 site. However, the calculated ratios deviate significantly from those established by chemical analysis for samples with higher Si/Al ratios. This is primarily

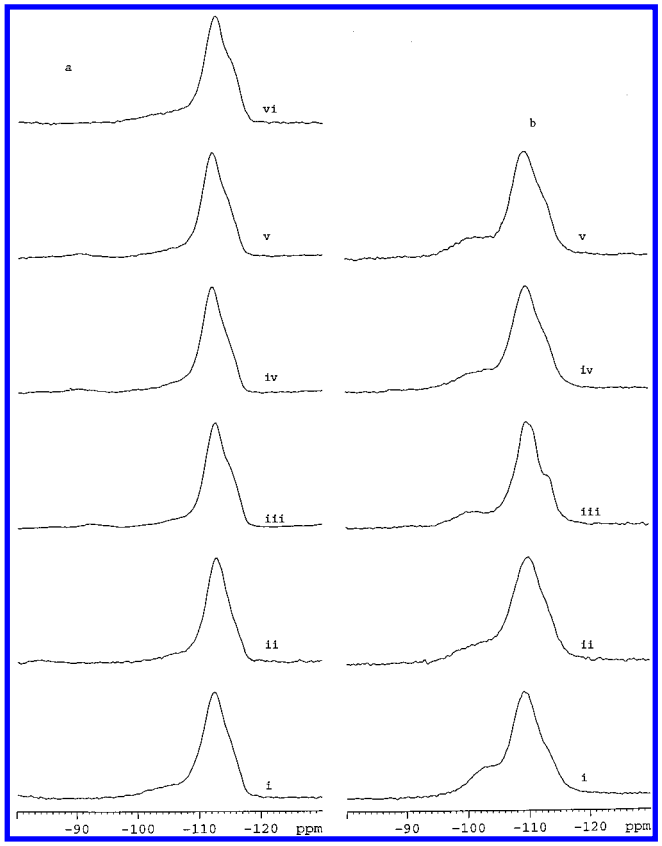

Figure 7. High-resolution Si-29 NMR (79.5 MHz) spectra of the ZSM-12 (a) and β zeolite (b) samples indicated by abbreviations i−vi in Figure 4.

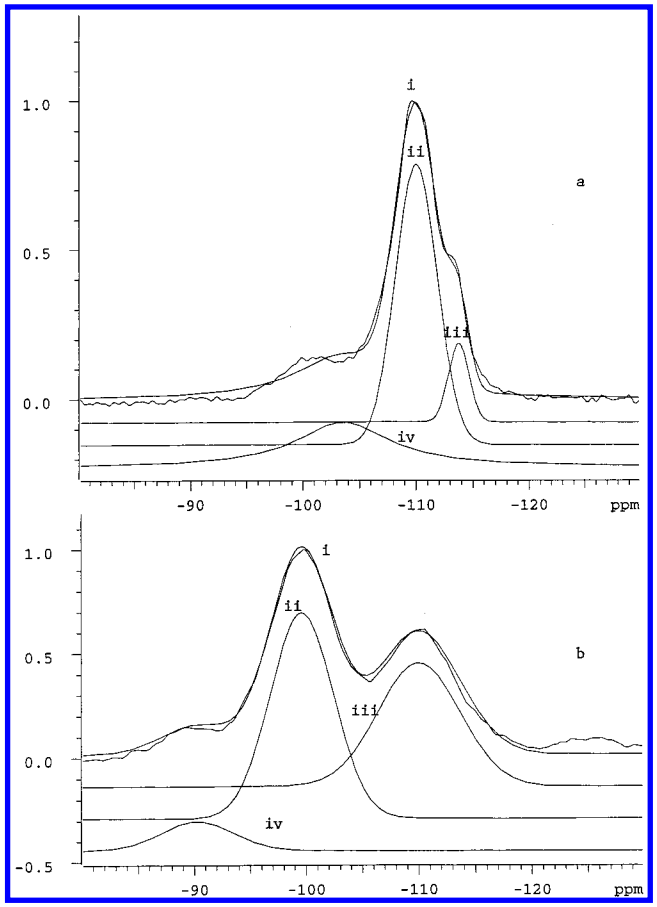

Figure 8. Experimental and simulated MAS Si-29 (a) and CP-MAS (b) spectra of a β zeolite (Si/Al = 70) sample. The simulated and experimental spectra are the two closely matched overlapped peaks abbreviated as i, with the smooth curve being the simulated one, and the calculated component peaks are labeled as ii, iii, and iv. Note that the peak from the CP-MAS experiment at −100 ppm appears at the same chemical shift as the Q^3 peak of the MAS experiment.

due to the fact that signals from Si−OH moieties overlap with the signal for the Q^3 sites. This overlapping feature has been demonstrated by performing CP-MAS experiments. Figure 8b shows the CP-MAS spectra of ZSM-12 samples. The spectra exhibit two peaks which are largely due to the magnetization transfer from proton to the silicon centers, and therefore they must contain SiOH functionalities. One of these peaks appears at the same chemical shift as that of the Q^3 site. Naturally, calculations based on the areas resolved from high-resolution MAS spectra cannot be meaningful in our samples with high Si/Al ratios since extensive dealumination is expected to release oxo centers which are readily converted to hydroxy species and we expect the Si−OH moiety to increase with increasing dealumination.

There has been considerable interest in defining the various Al sites in β zeolite. Both the aluminum and silicon NMR results described above should be discussed in the context of other studies performed on these two zeolites. On the basis of the charge and mass balance calculations as well as the observation of a new Al−O−H stretching frequency in the IR spectra, others[1] concluded that, in addition to the tetrahedral and octahedral Al sites, there are low-symmetry Al sites which were invisible by NMR spectroscopy. Indeed, such low-symmetry sites are expected to broaden the line width considerably, and in extreme cases, NMR signals may be invisible due to excessive broadening of signals. As indicated earlier, the broad asymmetric signal centered at 55 ppm can be decomposed to a signal of the usual line width of a tetrahedral site and another signal of much larger line width. The chemical shifts of these signals, however, are not remarkably different from each other. It is highly likely that, due to the defects in the framework created during the calcination process, some Al sites may deviate considerably from tetrahedral geometry yet maintain the same coordination number. Therefore, a larger line width compared to that of the regular tetrahedral site with a small change in chemical shift is expected. Furthermore, we did not observe any conversion of tetrahedral sites to the octahedral ones due to dealumination which was observed by other researchers. Although the broadening of peaks can be attributed to a number of factors,[18−25] including increased homo- and heteronuclear dipole−dipole interactions with quadrupolar nuclei, chemical shift anisotropy, thermal motions, and exchange processes, we believe the increased line width in the β zeolite is due to the presence of low-symmetry Al centers since ZSM-12 zeolite with comparable Si/Al ratios did not exhibit broader and asymmetric peaks.

Conclusions

Both ZSM-12 and β zeolites exhibit five different peaks which in general correspond to variable strength during the NH_3-STPD experiments. This technique provides a very accurate means of probing all the aluminum sites. We concluded that protonated zeolites possess distinct limits of acidity for both Lewis and Brønsted sites in contrast to other acidic supports. It was concluded that the increase of the extent of dealumination results in an increase of the acid strength for β zeolite and a decrease of the strength of ZSM-12. The FT-IR studies showed that both the as-synthesized and the dealuminated samples of β zeolite with Si/Al $\leq$ 80 possess Lewis sites. In contrast, only

the mother ZSM-12 sample possesses a relatively small amount of Lewis sites. The Al-27 MAS-NMR data also support the assumption that the former zeolite contained more octahedral aluminum sites compared to the ZSM-12 counterpart for samples with a Si/Al ratio below 40. Furthermore, there appear to be more distorted tetrahedral sites for β zeolite. In contrast to previous observations, the dealumination of ZSM-12 results in complete elimination of Lewis sites. It seems that the acid leaching with HCl "washes" completely the extraframework Al species.

Acknowledgment. The funding for this research from NSF through the Career Award (CTS-9702081) to P.G.S. and an instrumental grant from the Ohio Board of Regents to R.N.B. are gratefully acknowledged. Acknowledgment is made by P.G.S. to the donors of the Petroleum Research Fund, administered by the ACS, for support of this research through Grant ACS-PRF 31606-G5.

References and Notes

(1) Bourgeat-Lami, E.; Massiani, P.; Di Renzo, F.; Espiau, P.; Fajula, F. *App. Catal.* **1991**, *72*, 139.

(2) Remy, M. J.; Stanica, D.; Poncelet, G.; Feijen, E. J. P.; Grobet, P. J.; Martens, J. A.; Jacobs, P. A. *J. Phys. Chem.* **1996**, *100*, 12440.

(3) Woolery, G. L.; Kuehl, G. H.; Timken, H. C.; Chester, A. W.; Vartuli, J. C. *Zeolites* **1997**, *19*, 288.

(4) Jacobs, P. A.; Tielen, M.; Nagy, J. B.; Debras, G.; Derouane, E. G.; Gabelica, Z. In *Proceedings of the 6th International Zeolite Conference*, Reno, NV; Olson, D., Bisio, A., Eds.; Butterworths: Guildford, 1984; p 783.

(5) Robb, G. M.; Zhang, W.; Smirniotis, P. G. *Microporous Mesoporous Mater.* **1998**, *20*, 307.

(6) Mirodatos, C.; Ha, B. H.; Otsuka, K.; Barthomeuf, D. In *Proceedings of the 5th International Conference on Zeolites*; Rees, L. V., Ed.; Heyden: London, 1980; p 382.

(7) Post, J. G.; van Hooff, J. H. C. *Zeolites* **1984**, *4*, 9.

(8) Cvetanovic, R. J.; Amenomiya, Y. *Adv. Catal.* **1967**, *17*, 103.

(9) Cvetanovic, R. J.; Amenomiya, Y. *Catal. Rev.* **1972**, *6*, 21.

(10) Datka, J.; Gil.; B.; Kubacka, A. *Zeolites* **1995**, *15*, 501.

(11) Chen, D.; Sharma, S.; Cardona-Martinez, N.; Dumesic, J. A.; Bell, V. A.; Hodge, G. D.; Madon, R. J. *J. Catal.* **1992**, *136*, 392.

(12) Economidis, N. V.; Peña D. A.; Smirniotis, P. G. *Appl. Catal. B* **1999**, *23*, 123.

(13) Kofke, T. J. G.; Gorte, R. J.; Kokotailo, G. T.; Farneth, W. E. J. *J. Catal.* **1989**, *115*, 273.

(14) Zhang, W.; Burckle, E.; Smirniotis, P. G. *Microporous Mesoporous Mater.* **1999**, *33*, 173.

(15) Chiche, B. H.; Dutartre, R.; Di Renzo, F.; Fajula, F. Katovic, A.; Regina, A.; Giordano, G. *Catal. Lett.* **1995**, *31*, 359.

(16) Miller, J. T.; Hopkins, P. D.; Meyers, B. L.; Ray, G. J.; Roginski, R. T.; Zajac, G. W.; and Rosenbaum, N. H. *J. Catal.* **1992**, *138*, 115.

(17) Mueller, D.; Hoebbel, D.; Gessner, W. *Chem. Phys. Lett.* **1981**, *84*, 25.

(18) Andrew, E. R.; Jasinski, A. *J. Phys. Chem. Solid State Phys.* **1971**, *4*, 391.

(19) Alla, M.; Lippmaa, E. *Chem. Phys. Lett.* **1982**, *87*, 30.

(20) Freude, D.; Hunger, M.; Pfeifer, H.; Schwieger, W. *Chem. Phys. Lett.* **1986**, *128*, 62.

(21) Brunner, E. *J. Chem. Soc., Faraday Trans.* **1990**, *86*, 3957.

(22) Brunner, E.; Freude, D.; Gerstein, B. C.; Pfeifer, H. *J. Magn. Reson.* **1990**, *90*, 90.

(23) Li, D.; Bose, R. N. *J. Chem. Soc., Chem. Commun.* **1992**, 1596.

(24) Olivieri, A. C. *J. Magn. Reson.* **1993**, *101*, 313.

(25) Li, D.; Bose, R. N. *J. Chem. Soc., Dalton Trans.* **1994**, 3717.